Since January 2020 Elsevier has created a COVID-19 resource centre with free information in English and Mandarin on the novel coronavirus COVID-19. The COVID-19 resource centre is hosted on Elsevier Connect, the company's public news and information website.

Available online at www.sciencedirect.com
ScienceDirect
Virology 365 (2007) 435–445
VIROLOGY
www.elsevier.com/locate/yviro

Cell cycle arrest and apoptosis induced by the coronavirus infectious bronchitis virus in the absence of p53

Frank Q. Li [a,1], James P. Tam [a,c], Ding Xiang Liu [a,b,*]

[a] School of Biological Sciences, Nanyang Technological University, 60 Nanyang Drive, Singapore 637551, Singapore
[b] Institute of Molecular and Cell Biology, 61 Biopolis Drive, Proteos, Singapore 138673, Singapore
[c] The Scripps Research Institute, 5353 Parkside Drive, Jupiter, FL 33458, USA

Received 12 February 2007; returned to author for revision 4 March 2007; accepted 5 April 2007
Available online 9 May 2007

Abstract

Manipulation of the cell cycle and induction of apoptosis are two common strategies used by many viruses to regulate their infection cycles. In cells infected with coronaviruses, cell cycle perturbation and apoptosis were observed in several reports. However, little is known about how these effects are brought out, and how manipulation of the functions of host cells would influence the replication cycle of coronavirus. In this study, we demonstrate that infection with coronavirus infectious bronchitis virus (IBV) imposed a growth-inhibitory effect on cultured cells by inducing cell cycle arrest at S and G_2/M phases in both p53-null cell line H1299 and Vero cells. This cell cycle arrest was catalyzed by the modulation of various cell cycle regulatory genes and the accumulation of hypophosphorylated RB, but was independent of p53. Proteasome inhibitors, such as lactacystin and NLVS, could bypass the IBV-induced S-phase arrest by restoring the expression of corresponding cyclin/Cdk complexes. Our data also showed that cell cycle arrest at both S- and G_2/M-phases was manipulated by IBV for the enhancement of viral replication. In addition, apoptosis induced by IBV at late stages of the infection cycle in cultured cells was shown to be p53-independent. This conclusion was drawn based on the observations that apoptosis occurred in both IBV-infected H1299 and Vero cells, and that IBV infection did not affect the expression of p53 in host cells.

Keywords: Cell cycle arrest; Apoptosis; Coronavirus IBV; p53-independent

Introduction

Host factors are involved in all steps of the viral replication cycle. Concomitantly, host gene expression and anti-viral defense mechanisms are modulated by viruses in order to optimize their own replication. Two aspects of such regulations with increasing importance are the viral manipulation of the progression of host cell cycle and apoptosis. Cell cycle progression is triggered by the activation of a series of cyclin-dependent kinases (Cdks), which form complexes with cyclins, and are regulated by the availability of the cyclin subunit, changes in phosphorylation state, and association with cellular Cdk inhibitors (CKIs), such as $p21^{Cip1}$, $p27^{Kip1}$, p^{57Kip2}, and $p16^{ink4a}$, whose expression is also tightly controlled (Morgan, 1995; Nurse, 2004; Sherr and Roberts, 1999). Viruses may manipulate host cell cycle to maximize their own replication. Apoptosis constitutes part of the host cell defense mechanisms against viral infection (Benedict et al., 2002; Hay and Kannourakis, 2002). Viral infection could activate a variety of signal transduction pathways that lead to apoptosis of the infected cells. A number of viruses and their gene products were found to be able to induce apoptosis (Roulston et al., 1999; Teodoro and Branton, 1997). Apoptosis can also facilitate the release of progeny virus and thus plays important roles in the viral life cycle during a lytic infection (Roulston et al., 1999). In this report, we study the cell cycle manipulation and induction of apoptosis in cells infected with coronavirus using avian infectious bronchitis virus (IBV) as a model system.

Coronaviruses are a diverse group of large, enveloped, single-stranded and positive-sense RNA viruses which cause a

* Corresponding author. Institute of Molecular and Cell Biology, 61 Biopolis Drive, Proteos, Singapore 138673, Singapore. Fax: +65 67791117.
E-mail address: dxliu@imcb.a-star.edu.sg (D.X. Liu).
[1] Current address: Department of Laboratory Medicine, University of Washington Medical Center, 325 9th Ave, Seattle, WA 98104, USA.

0042-6822/$ - see front matter © 2007 Elsevier Inc. All rights reserved.
doi:10.1016/j.virol.2007.04.015

variety of economically important diseases affecting humans and animals (Lai and Holmes, 2001). In 2003, severe acute respiratory syndrome coronavirus (SARS-CoV) emerged as a dangerous pandemic agent that caused a highly contagious health threat with a fatality rate of 10% (Ksiazek et al., 2003). IBV, the prototype of coronavirus, is the etiological agent of infectious bronchitis which impairs the respiratory and urogenital tracts of chickens. Recently, a number of reports highlighted that coronaviruses and their encoded proteins could induce cell cycle perturbation. Murine coronavirus mouse hepatitis virus (MHV) and its nonstructural protein p28 were shown to induce G_0/G_1 arrest (Chen and Makino, 2004; Chen et al., 2004a). The nucleocapsid (N) protein of SARS-CoV disrupts cytokinesis and blocks S-phase progression in mammalian cells by inhibiting the activity of cyclin–Cdk complex (Li et al., 2005; Surjit et al., 2006), and SARS-CoV infection increased the number of hepatocytes undergoing mitosis (Chau et al., 2004). Various coronaviruses and their encoded proteins were also found to be inducers of apoptosis. These include both structural and nonstructural proteins of SARS-CoV (Chau et al., 2004; Chow et al., 2005; Law et al., 2005; Surjit et al., 2004; Tan et al., 2004; Yang et al., 2005), IBV (Liu et al., 2001), TGEV (Eleouet et al., 1998), and MHV (Liu et al., 2003) and its E protein (An et al., 1999). However, the involvement of p53, which is a key mediator of apoptosis, has never been reported.

During the preparation of this paper, a study reported that infection of Vero cells with IBV could induce G_2/M cell cycle arrest (Dove et al., 2006). However, little is known about how these effects are brought out, and how the growth state of host cells influences coronavirus replication. In this study, we demonstrated that IBV infection imposed a growth-inhibitory effect on cultured cells by inducing cell cycle arrest at both S and G_2/M phases. The arrest was catalyzed by modulation of various cell cycle regulatory genes and the accumulation of hypophosphorylated RB, but was independent of p53 status of the host cells. Proteasome inhibitors, such as lactacystin and NLVS, could bypass the S-phase arrest by restoring the expression of corresponding cyclin–Cdk complexes. Moreover, arrest at both S- and G_2/M-phases by IBV could enhance viral replication. Meanwhile, induction of caspase-dependent apoptosis in both p53-null H1299 cells and wild-type p53-containing Vero cells was examined, showing that IBV explores a p53-independent mechanism to induce apoptosis in cultured mammalian cells.

Results

Inhibition of cell proliferation by IBV infection of H1299 and Vero cells

It was reported that IBV infection of p53-containing Vero cells resulted in cell cycle arrest at G_2/M phase (Dove et al., 2006). To rule out the possibility that this cell cycle arrest is Vero cell-specific, search for other cell lines that are susceptible to the Vero cell-adapted IBV was carried out, resulting in the selection of a number of cell lines that support efficient IBV infection (data not shown). Among them, H1299, a human lung carcinoma cell line, was used in this study. Similar to the typical cytopathic effects (CPE) in Vero cells, IBV infection of H1299 cells showed rounding up and fusion of infected cells to form giant multinucleated syncytia, detachment of infected cells from the culture dish, and eventually cell lysis and death (Fig. 1a). The infected cells were further analyzed by Western blot with anti-IBV N protein antibodies. A typical N protein profile was detected (Fig. 1a). These results confirm that the Vero cell-adapted IBV could efficiently infect H1299 cells. As H1299 is a p53-null cell line (Gjoerup et al., 2001), it also provides a good cell system for studying the involvement of p53 in IBV-induced cell cycle arrest and apoptosis.

The effect of IBV infection on host cell proliferation was then tested by infection of H1299 and Vero cells with IBV at MOI of 0.5 (IBV-I) and 1 (IBV-II), respectively, in a time course experiment. Determination of total cell number showed that IBV inhibited cell growth in an MOI- and time-dependent manner (Fig. 1b). The reduction in cell number for H1299 cells was more significant than that of Vero cells (Fig. 1b). Further analysis of cell proliferation by MTT assay showed that, at a MOI of 1, IBV infection inhibited the growth of both cell lines efficiently, although H1299 cells were more sensitive to IBV infection (Fig. 1c). These results demonstrate that IBV infection inhibits cell proliferation, and the p53 status is not a determinant for IBV-mediated growth inhibition. However, p53 might play a certain role, as more obvious inhibition of growth was observed in p53-null cells.

Induction of aberrant cell cycle progression in IBV-infected H1299 and Vero cells

The cell cycle profiles in IBV-infected H1299 and Vero cells were then analyzed. Asynchronously growing H1299 and Vero cells were infected with IBV, harvested at different time points post-infection, and the nuclear DNA was stained with propidium iodide (PI) before analysis by flow cytometry (FACS). For both cell lines, slight increase (3%–10%) of S-phase cells was observed at 6 and 12 h post-infection (Fig. 2, upper panels). The S-phase cells were increased by 7%–10% in IBV-infected Vero cells at 18 and 24 h post-infection, and further increased by 20% at 30 h post-infection (Fig. 2, upper panels). Much higher degree of increase (20%–30%) of S-phase cells was observed at the same time points in IBV-infected H1299 cells (Fig. 2, upper panel). Accumulation of G_2/M-phase cells at the level of 15% and 6%, respectively, was also observed in IBV-infected Vero cells at 18 and 24 h post-infection (Fig. 2, upper panel). The accumulation of cells in the G_2/M phase was only observed at 30 h post-infection in IBV-infected H1299 cells (Fig. 2, upper panel).

The cell cycle perturbation induced by IBV infection was further investigated using synchronized H1299 and Vero cells in the quiescent state by serum deprivation prior to infection. The cell cycle progression was re-started by serum stimulation and cells were subjected to FACS analysis. The cell cycle profiles of IBV-infected H1299 and Vero cells showed comparable levels of arrest at both S (10%–30%) and G_2/M (5%–15%) phases

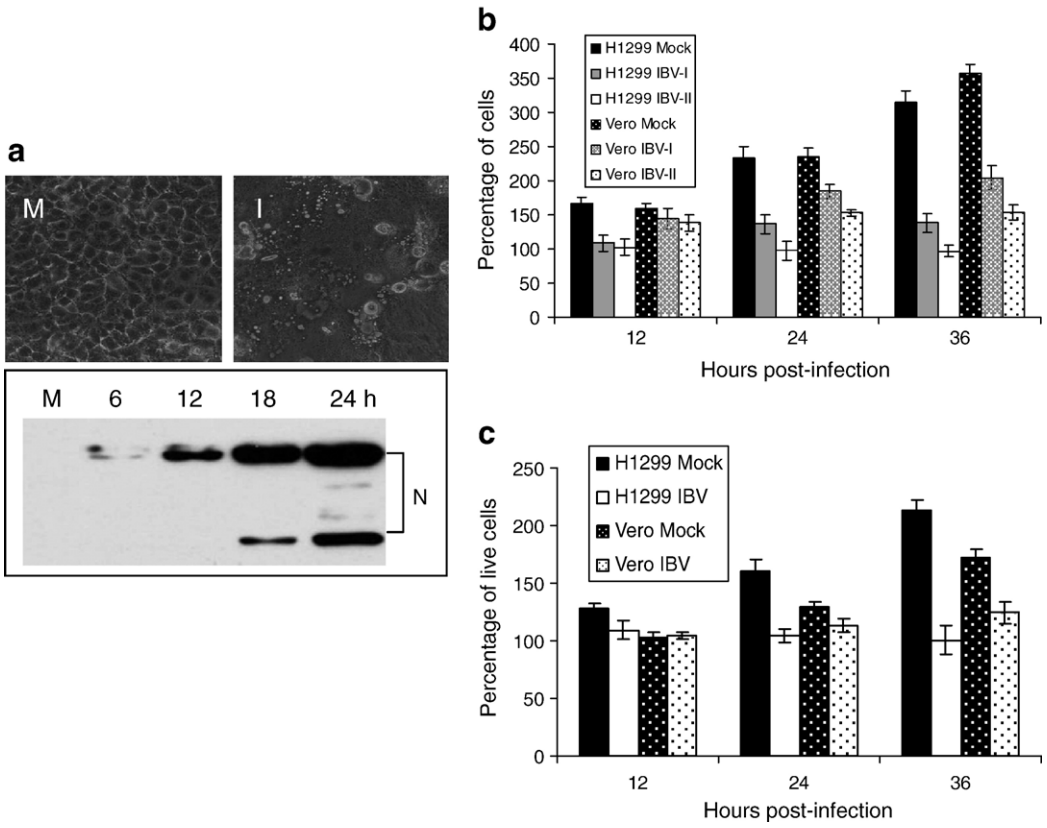

Fig. 1. Inhibition of cell proliferation in IBV-infected H1299 and Vero cells. (a) H1299 cells were mock (M) or infected with IBV (I) at an MOI of 1. The morphological characteristics of the infected cells were observed under a light microscope at 36 h post-infection (upper panels). At the indicated times, cells were lysed with SDS sample buffer and viral protein expression was tested by Western blot analysis with anti-IBV N polyclonal antibodies. (b) H1299 and Vero cells at 50% confluence in 6-well plates were infected with IBV at an MOI of 0.5 (IBV-I) or 1 (IBV-II). At various times post-infection, the total cell numbers were counted and plotted. Data are presented as percentage of cell numbers compared with that of mock-infected cells at 0 h post-infection. The percentages are results of five repeated experiments. (c) Analysis of cell proliferation by MTT assay. H1299 and Vero cells at 50% confluence in 96-well plates were mock- or IBV-infected at an MOI of 1. At various times post-infection, MTT assays were performed. Data are presented as percentage of live cells compared with that of mock-infected cells at 0 h post-infection. The percentages are results of five repeated experiments.

with those of asynchronously growing cells (Fig. 2, lower panel).

FACS analysis also revealed that IBV infection selectively induced cell cycle entry in H1299 cells. Analysis of cell cycle profiles showed that IBV infection remarkably decreased the proportion of G_0/G_1-phase cells and significantly increased the number of S-phase cells (Fig. 2, lower panel). Prior to infection, approximately 83% of serum-starved cells were arrested at the G_0/G_1 phase. At 12 and 18 h post-infection, respectively, 6% and 24% decrease of G_0/G_1-phase population and 12% and 24% increase of S-phase population were observed in mock-infected cells (Fig. 2, lower panel). However, much more dramatic decrease (17% and 39%) of G_0/G_1-phase cells and increase (22% and 42%) of S-phase cells were observed in IBV-infected cells at the same time points (Fig. 2, lower panel). Similar phenomena were also seen in quiescent Vero cells (Fig. 2, lower panel).

Analysis of cell cycle-related genes in IBV-infected H1299 and Vero cells

As progression through the cell cycle is mediated by Cdks complexed with corresponding cyclins, the possibility that IBV infection would modulate such cell cycle regulators at the protein level was investigated. Western blot analysis of various Cdks and cyclins were first carried out in IBV-infected H1299 cells. At 12 h post-infection, cyclins B1 and E was 2-fold higher in IBV-infected cells than that in mock-infected cells (Fig. 3a, lanes 2 and 3). However, a marginal decrease of Cdk2 was observed in IBV-infected cells, while cyclins A and D1 as well as Cdk1 were unchanged (Fig. 3a, lanes 2 and 3). At 18 h post-infection, the expression of Cdk2 and cyclin D1 was decreased 2- and 3-fold, respectively, in IBV-infected cells, but cyclins A, B1, E and Cdk1 were almost identical between mock-infected and IBV-infected cells (Fig. 3a, lanes 4 and 5). A 3-fold reduction of cyclins A, B1 and D1, and a 2-fold reduction of Cdk 1 and Cdk2 were observed in IBV-infected cells at 24 h post-infection (Fig. 3a, lanes 6 and 7). More drastic reduction of cyclins A and D1 (5- and 10-fold) and Cdk1 (3-fold) was observed in IBV-infected cells at 30 h post-infection (Fig. 3a, lanes 8 and 9).

In parallel experiments, Western blot analysis of the expression of these Cdks and cyclins in IBV-infected Vero cells showed generally more drastic reduction in the expression of these proteins than in IBV-infected H1299 cells (Fig. 3a,

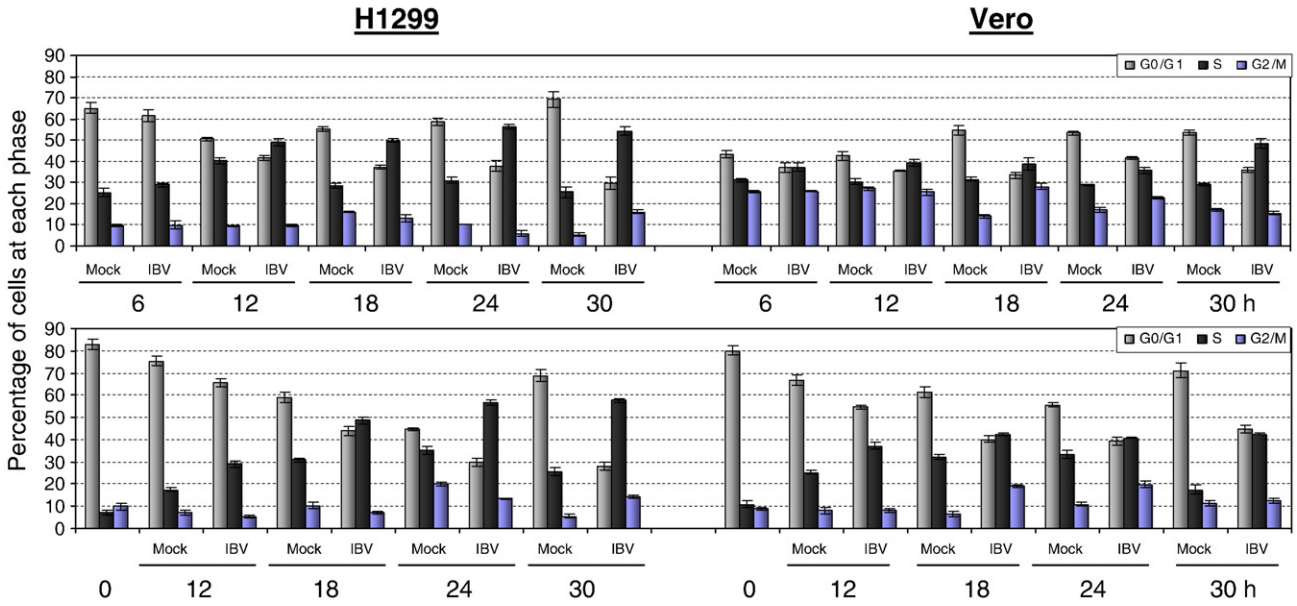

Fig. 2. Induction of aberrant cell cycle progression in IBV-infected cells. H1299 and Vero cells were infected with IBV at an MOI of 1. At the indicated times, cells were collected and stained with propidium iodide for FACS analysis. Data were analyzed by using the ModFit LT Mac 3.0 software to determine the percentage of cells at each phase of the cell cycle in both asynchronously growing (upper panels) and synchronized (lower panels) H1299 and Vero cells. The results are presented as means of five repeated experiments.

lanes 10–18). Among them, the most prominent were cyclins B1 and Cdk2 (2- and 5-fold lower) (Fig. 3a). The replication of IBV in both cell lines was monitored by Western blot analysis of the IBV N protein, showing that the expression of N protein was gradually increased over time (Fig. 3a). In both IBV-infected H1299 and Vero cells, the nucleolar protein fibrillarin as well as β-tubulin remained constant (Fig. 3a).

The phosphorylation status of RB in IBV-infected H1299 cells was then examined by Western blot analysis. In mock-infected cells, only the hyperphosphorylated form of RB (ppRB)

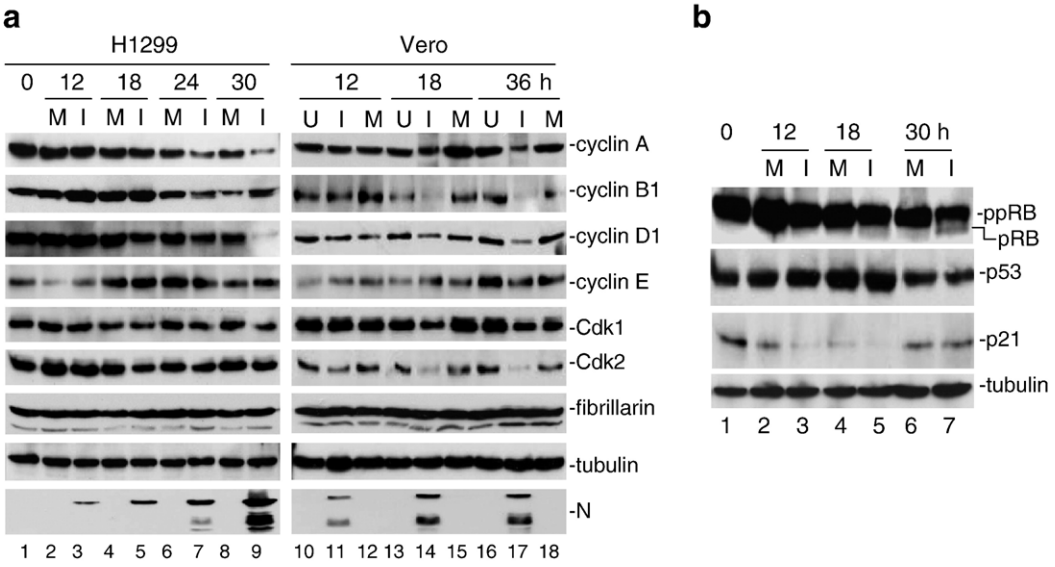

Fig. 3. Western blot analysis of cell cycle-related genes. (a) H1299 (left panels) and Vero (right panels) cells were either uninfected (U), mock-infected (M) or infected with IBV (I) at an MOI of 1. At the indicated times, cells were lysed with SDS sample buffer, and equal amounts of proteins from the samples were tested by Western blot analysis with anti-cyclins A, B1, D1, and E, Cdk1, Cdk2, and fibrillarin antibodies, respectively. The same membranes were also probed with β-tubulin as a loading control. Viral replication was confirmed by Western analysis of N protein with anti-IBV N polyclonal antibodies. The data were representatives of three repeated experiments. (b) Asynchronously growing H1299 (top panel) and Vero (other panels) cells were infected with IBV at an MOI of 1 (I). At the indicated times, cells were lysed and subjected to Western blot analysis with anti-RB, p53, p21 and β-tubulin antibodies, respectively. Hypophosphorylated forms of RB (pRB) appeared as fast-migrating bands, and hyperphosphorylated RB (ppRB) appeared as slightly retarded bands (top panel). The data are representative of three independent experiments.

was detected (Fig. 3b, lanes 2, 4 and 6). No obvious detection of the minor hypophosphorylated RB (pRB) was seen (Fig. 3b, lanes 2, 4, and 6). In IBV-infected cells, pRB was detectable at 18 h post-infection and was accumulated to a higher level at 30 h post-infection (Fig. 3b, lanes 5 and 7). It was also noted that less ppRB was detected in IBV-infected cells at 30 h post-infection (Fig. 3b, lane 7), indicating that the cells were not able to progress through the cell cycle smoothly.

We finally examined whether IBV infection of Vero cells could induce p53 expression and the accumulation of p21. The results showed that there was no obvious difference in both the overall expression level and the post-translational modification of p53 between mock- and IBV-infected cells throughout the time-course experiment (Fig. 3b). The p21 expression was reduced by 3- and 4-fold in IBV-infected cells at 12 and 18 h post-infection, respectively, compared to that in mock-infected cells. However, the expression of p21 was identical in both groups at 30 h post-infection (Fig. 3b). These data suggest that IBV-induced cell cycle arrest was independent of the activation of p53 and p21.

Bypass of IBV-induced S-phase arrest in cells treated with proteasome inhibitors

As IBV infection induced concomitant inhibition of S-phase progression and G_2/M transition through down-regulation of various cell cycle regulatory proteins including cyclins A, B1 and D1 as well as Cdk1 and Cdk2, the underlying mechanisms were then investigated. As cyclin A, Cdk2 and cyclin D1 were reported to be degraded through ubiquitin-dependent proteolysis pathway in tumor cells and in cells infected with coxsackievirus (Chen et al., 2004b; Luo et al., 2003), Western blot analysis of these proteins were carried out in IBV-infected H1299 cells in the presence of proteasome inhibitors, lactacystin and NIP-leu-leu-leu-vinyl-sulfone (NLVS). As can be seen in Fig. 4a, IBV infection induced a 22% increase of S-phase cells at 24 h post-infection (compared 'Mock' with 'DMSO'). Addition of both lactacystin and NLVS annulled the S-phase cell cycle arrest and restored the expression of cyclin A, Cdk2 and cyclin D1 protein in a dose-dependent manner (Figs. 4a and b). Lactacystin was shown to be more efficient than NLVS, except in the stabilization of cyclin A (Figs. 4a and b). The effectiveness of the proteasome inhibitors was also proved by the accumulation of multiubiquitinated proteins (Fig. 4b). The level of Cdk1 remained unchanged under identical experimental conditions (Fig. 4b). These data suggest that IBV infection specifically promotes the degradation of cyclin A, Cdk2 and cyclin D1 through a proteasome-dependent mechanism, leading to the cell cycle arrest.

Effects of cell cycle arrest at S and G_2/M phases on IBV replication

Manipulation of cell cycle progression is an important strategy exploited by many viruses to create conducive cellular conditions for viral replication. To determine the effect of cell

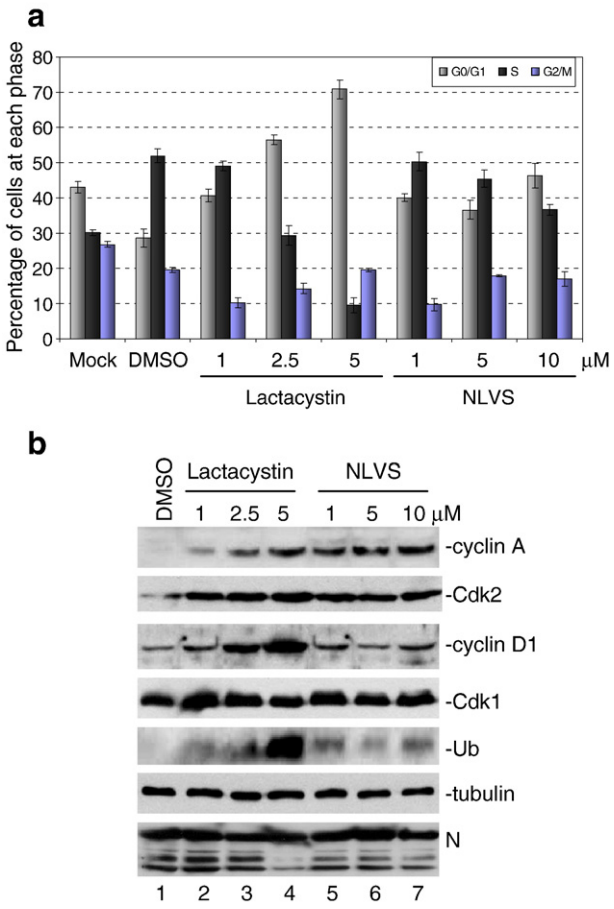

Fig. 4. Bypass of IBV-induced S-phase arrest in cells treated with proteasome inhibitors. (a) Vero cells were preincubated with either DMSO or increasing concentrations of proteasome inhibitors, lactacystin and NLVS, for 30 min and then infected with IBV. At 24 h post-infection, the cells were collected and subjected to FACS analysis. The data are presented as means of three repeated experiments. (b) Cell lysates were analyzed for cyclin A, D1, Cdk1, Cdk2, ubiquitin, β-tubulin, and IBV N protein by Western blotting. The data are representative of three independent experiments.

cycle arrest on IBV replication, H1299 cells were synchronized with methotrexate to create an S-phase environment, and the viral production in these cells was determined by titration and Western blot analysis of IBV N protein. Accordingly, asynchronously growing H1299 cells were treated with either DMSO or methotrexate for 20 h, followed by incubation in fresh medium for 6 h to release the cell cycle progression. After release, more than 65% of the cells in the methotrexate-treated group entered the S phase (Fig. 5a). Cells treated with DMSO or methotrexate were infected with IBV and harvested at 24 and 48 h post-infection, respectively. Determination of the $TCID_{50}$ of viruses harvested at 24 and 48 h post-infection, respectively, showed that approximately 7- and 11-fold more viruses were produced from the methotrexate-treated cells (Fig. 5a, lower panel). Western blot analysis confirmed that higher expression of the N protein was detected in cells treated with methotrexate at 24 h post-infection (Fig. 5c, lanes 1–4).

The effect of cell cycle arrest at the G_2/M phase on IBV replication was then tested. Asynchronously growing H1299

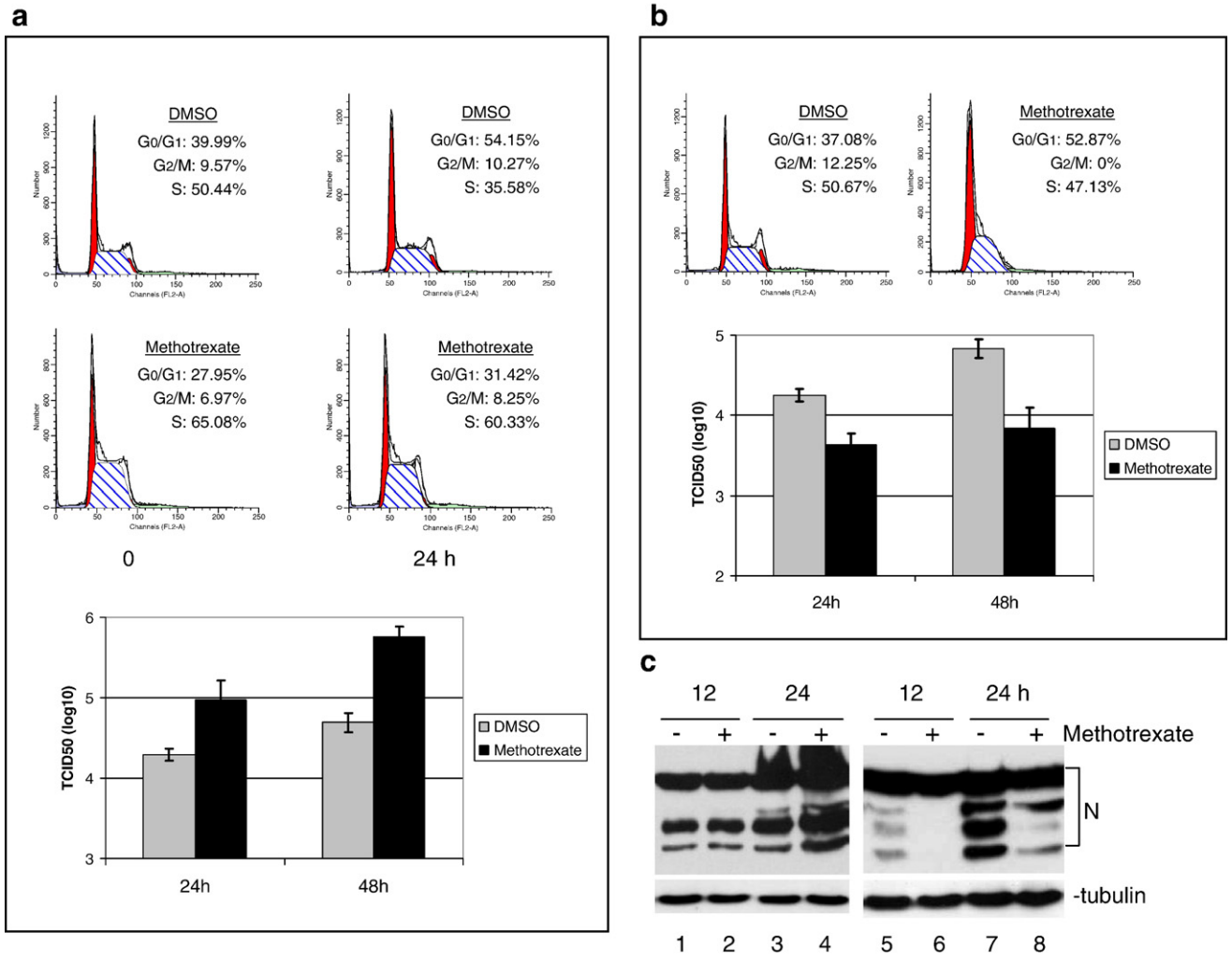

Fig. 5. S and G_2/M arrest promotes IBV replication. (a) Asynchronously growing H1299 cells were treated with DMSO or methotrexate for 20 h, followed by incubation in fresh medium for 6 h to release the cell cycle progression. Cells were then infected with IBV at an MOI of 1 and harvested at 24 and 48 h post-infection, and viral titers were determined (bottom panel). The cell cycle profiles at the end of fresh medium incubation and 24 h post-infection were analyzed by flow cytometric analysis (top and middle panels). (b) Asynchronously growing H1299 cells were mock-infected or infected with IBV at an MOI of 1, followed by incubation with either DMSO or methotrexate. The cell cycle profiles at 24 h post-infection were obtained by flow cytometric analysis (upper panels). Viral titers at 24 and 48 h post-infection were determined (lower panel). (c) Viral protein expression at 12 and 24 h post-infection was analyzed by Western blot with anti-IBV N polyclonal antibodies.

cells were infected with IBV, followed by incubation with methotrexate. Treatment with methotrexate blocks the replicating cells at the G_1/S border, leading to a total loss of cells in the G_2/M phase, while the percentage of cells in the S phase remained unchanged (Fig. 5b). Cells were harvested at 12, 24 and 48 h post-infection, and the viral titers were determined. The results showed that approximately 7- and 10-fold less viruses were produced from cells treated with methotrexate at 24 and 48 h post-infection, respectively (Fig. 5b, lower panel). Western blot analysis confirmed that lower expression of the N protein in cells treated with methotrexate at 12 and 24 h post-infection (Fig. 5c, lanes 5–8).

Induction of p53-independent apoptosis by IBV

In a previous study, it was reported that IBV infection induced caspase-dependent apoptosis in cultured cells (Liu et al., 2001). To further elucidate the molecular mechanisms by which IBV induces apoptosis, especially the potential requirement of p53 in IBV-induced apoptosis, both p53-null H1299 cells and wild-type p53-containing Vero cells were infected with IBV, and the extent of genomic DNA fragmentation, i.e. the occurrence of the characteristic nuclear hypodiploid DNA content, was analyzed by FACS. A substantial increase in the number of apoptotic cells was observed at 36 h post-infection in both cell lines (Fig. 6a). Nuclear staining with Hoechst showed apparently distorted and fragmented nuclei (Fig. 6b). As the TUNEL assay could distinguish apoptotic cells undergoing DNA fragmentation by adding labeled nucleotides to the fragmented DNA ends, cells even at early stages of apoptosis could be visualized by horseradish peroxidase colorimetric reaction. As shown in Fig. 6b, the number of TUNEL signal-positive cells was drastically increased at 36 and 48 h post-infection in both cell lines (Fig. 6b). Addition of the broad caspase inhibitor, QVD, significantly reduced the detection of the TUNEL signal-

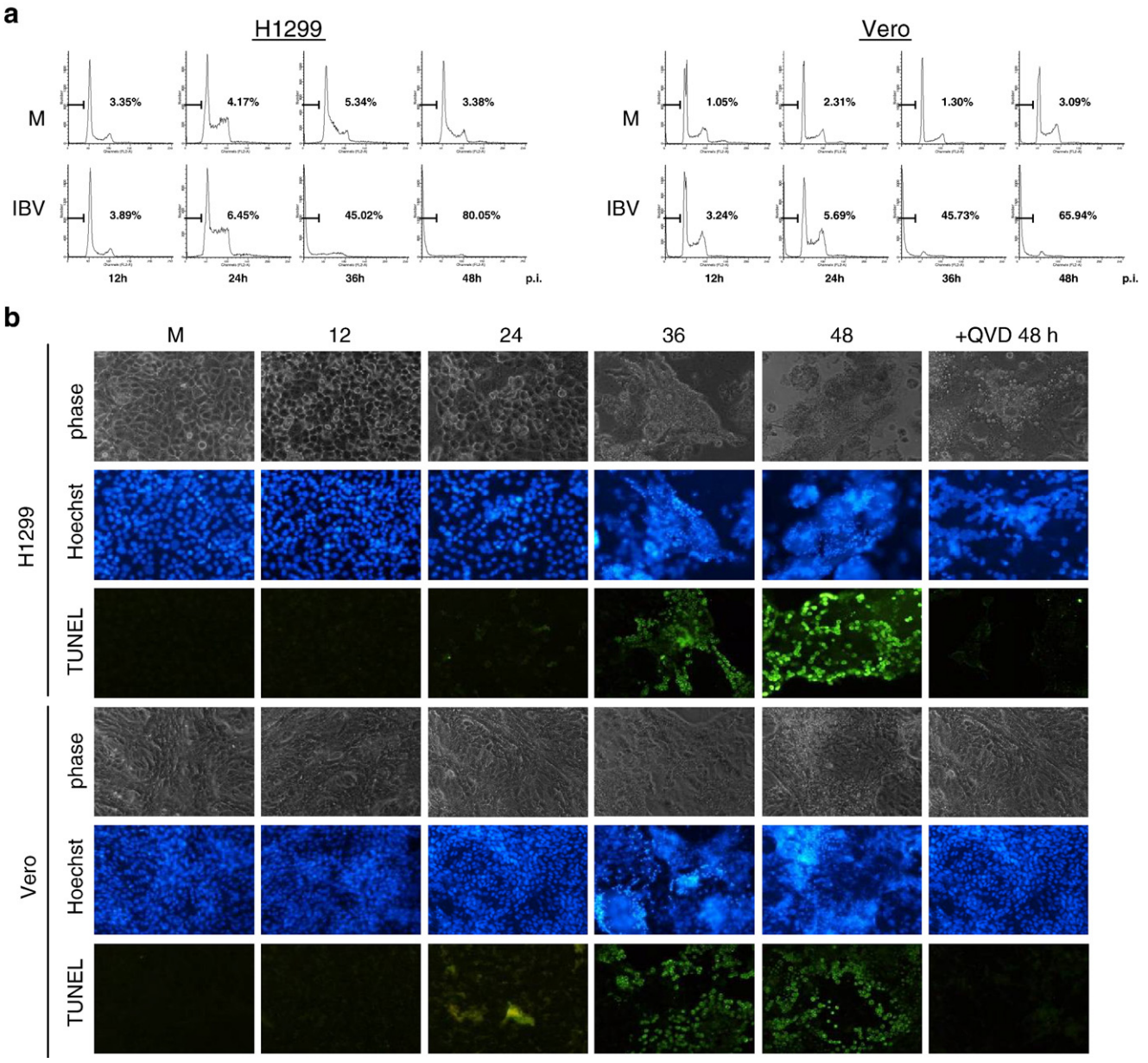

Fig. 6. Induction of apoptotic cell death in IBV-infected H1299 and Vero cells. (a) H1299 and Vero cells were infected with IBV at an MOI of 1. At the indicated times post-infection, cells were collected and stained with propidium iodide for flow cytometric analysis. Cells with sub-G_0/G_1 (hypodiploid) DNA contents are indicated by a bar and as percentage in each graph. The data are representative of three independent experiments. (b) Morphological characteristics and TUNEL assays of mock- and IBV-infected H1299 and Vero cells at 12, 24, 36, and 48 h post-infection. Cells were mock- or IBV-infected, stained with Hoechst 33342 or analyzed by TUNEL assay with an *in situ* cell death detection kit at the indicated times post-infection, and viewed under a fluorescence microscope. At 48 h post-infection, IBV-infected cells treated with a caspase inhibitor, QVD, were also analyzed by the same assays. The data are representative of three independent experiments. Phase, phase-contrast images; Hoechst, nuclear staining; TUNEL, TUNEL assay.

positive cells. These data strongly suggest that IBV infection is capable of inducing apoptosis irrespective of the presence or absence of functional cellular p53.

Discussion

Cell cycle manipulation and induction of apoptosis are two crucial events occurred in cells infected with many viruses. In this study, we demonstrate that IBV infection induces cell cycle arrest at the S and G_2/M phases at early stages and apoptosis at late stages of the viral infection cycle on cultured mammalian cells. The cell arrest at the S and G_2/M phases was catalyzed by viral modulation of various cell cyclins/Cdks and the accumulation of hypophosphorylated RB. Our data also showed that cell cycle arrest was manipulated by IBV for the benefit of viral replication. As IBV-induced cell cycle arrest and apoptosis were detected in both p53-null H1299 cells and wild-type p53-containing Vero cells, p53 activation is not required for the two events. This study not only extends the observations of Dove et al. (2006) to another cell type, but also reveals that IBV

infection could induce more extensive perturbation of cell cycle progression.

For successful propagation, viruses may manipulate cell cycle progression to create a more conducive environment (Op De Beeck and Caillet-Fauquet, 1997; Schang, 2003; Swanton and Jones, 2001). As cellular components fluctuate during the cell cycle, these manipulations may force the cell into a phase that is favorable for virus replication. In the case of DNA viruses, coordination with host cell DNA replication in the S phase may be required for efficient replication of the viral DNA genomes (Schang, 2003). For example, EBV could block the host response and actively promote an S-phase-like environment for viral lytic replication (Kudoh et al., 2004, 2005). S-phase-dependent enhancement of viral RNA replication was also reported for dengue virus 2 and hepatitis C virus (Helt and Harris, 2005; Scholle et al., 2004). Cell cycle dependence for retrovirus replication may include arrest at the S phase and mitosis (Katz et al., 2005). G_2/M arrest is also a common strategy employed by viruses to optimize virion production. Cell cycle arrest at G_2/M phase was observed to boost both early and late steps of HIV infection (Goh et al., 1998; Groschel and Bushman, 2005). Coxsackievirus, however, replicates more slowly in cells arrested at G_2/M, compared to cells arrested at either G_1 or the G_1/S boundary (Feuer et al., 2002). In this study, we demonstrated that IBV could manipulate cell cycle for the enhancement of viral replication. The G_2/M arrest may result in a change in the cellular physiology that is more conducive to viral infection. It is also possible that a simple increase in cell surface area due to arrest would promote viral entry. Furthermore, protein synthesis is greater in the G_2/M phase, which may have a knock-on effect on virus assembly and hence increase virus output.

Expression of both S and G_2 cyclins (A and B1) was down-regulated in IBV-infected cells. Interestingly, G_1 cyclins (D1 and E) were also degraded. Cyclin A, D1 and Cdk2 were proved to be destroyed in IBV-infected cells through ubiquitin-mediated proteolysis. The reduced levels of cyclin E, B1 and Cdk1, which are all target genes of the E2F transcription factors, could be attributed to the accumulation of active RB. The active Rb may restrain S-phase entry and target genes required for DNA replication largely by repressing the E2F activity (DeCaprio et al., 1989; Dyson, 1998; Harbour and Dean, 2000; Weinberg, 1995).

Modulation of the activity of p53 is a key event in the replication of many DNA viruses. In cellular response to viral infection, p53 is generally activated to induce either cell cycle arrest or apoptosis. As a DNA damage response protein, p53 transcriptionally activates numerous genes involved in apoptosis, DNA repair and cell cycle arrest (Vogelstein et al., 2000), and p53-dependent arrest of cells at G_1/S or G_2/M is an important component of the cellular response to genotoxic stress including virus infection. The first transcriptional target of p53 identified was p21, a CKI of the Cip/Kip family, which bridges the function of p53 with the cell cycle and plays important roles in regulation of cell cycle progression or arrest (el-Deiry et al., 1993; Harper et al., 1993). Overexpression of p21 could inhibit two critical checkpoints in the cell cycle, namely G_1 and G_2, through both p53-dependent and -independent pathways (Macleod et al., 1995). The observation that IBV infection induces cell cycle arrest at S and G_2/M phases in both H1299 and Vero cells virtually rules out the possible involvement of p53 in these processes.

IBV infection induces apoptosis in both H1299 and Vero cells, suggesting that IBV-induced apoptosis may also be p53-independent. To support this conclusion, neither p53 overall expression level nor its post-translational modification state was affected upon IBV infection. Viral proteins from several DNA viruses, including the SV40 small t antigen (Gjoerup et al., 2001), the Rep78 protein from adeno-associated virus type 2 (Schmidt et al., 2000), adenovirus E4orf4 protein (Kleinberger, 2000), HPV E6 (Fan et al., 2005), papillomavirus E2 (Desaintes et al., 1999) and the chicken anemia virus protein apoptin (Teodoro et al., 2004), were reported to induce p53-independent apoptosis. Induction of early apoptosis could limit viral production and spread of progeny virus to the neighboring cells, most viruses have therefore evolved strategies to disrupt early apoptosis to allow production of more progeny viruses. These include suppression of the IFN action in the case of human adenovirus and HPV (Barber, 2001), inactivation of p53 and coding for antiapoptotic Bcl-2 homologs to prevent premature death of the infected cells to sustain virus replication (Benedict et al., 2002; Cuconati and White, 2002). Some viruses or viral proteins, such as HTLV-1 Tax protein and HIV-1 Nef, inhibit apoptosis by modulating Bcl-2 family members at the transcriptional level or via post-translational modification (Benedict et al., 2002). Poxviruses, myxoma virus, human CMV, and adenovirus can specifically target members of the TNF receptor (Benedict et al., 2002).

Cross talk exists between cell cycle regulation and apoptosis (Gil-Gomez et al., 1998; King and Cidlowski, 1998). Apoptosis is an end point of stalled cell cycle progression in most cases. But in other cases, progression through the cell cycle appears to be required for efficient induction of apoptosis (Santiago-Walker et al., 2005). One characteristic feature of DNA damage-induced apoptosis, especially in the absence of wild-type p53, is the activation of a G_2/M cell cycle checkpoint prior to cell death. However, G_2/M cell cycle arrest is not always a prerequisite for subsequent apoptosis. Moreover, it was reported that apoptosis is frequently associated with the G_1 phase of the cell cycle (King and Cidlowski, 1998) and arrest at the late G_1 or S phase may accelerate or potentiate apoptosis (Meikrantz et al., 1994). In addition, apoptosis is a consequence of the S-phase arrest imposed by IFN-β in HPV-infected cervical carcinoma cell line ME-180 (Vannucchi et al., 2005). In this study, apoptosis may mechanistically link to the cell cycle arrest induced by IBV infection, but it is unlikely that apoptosis is merely a direct consequence of the cell cycle arrest. It is possible that cell cycle arrest in IBV-infected cells would prevent the induction and execution of early cell death of the infected cells.

Materials and methods

Viruses and cells

African green monkey kidney cell line Vero which carries wild-type p53 gene (Shivakumar et al., 1995) and p53-null human lung carcinoma cell line H1299 were obtained from the American Type Culture Collection (ATCC) and cultured in complete Dulbecco's modified Eagle's medium (DMEM) (Gibco) or RPMI 1640 (Hyclone) supplemented with 10% newborn calf serum (Sterile) and 1% penicillin/streptomycin (Invitrogen) and maintained at 37 °C in humidified 5% CO_2.

The Beaudette strain of IBV (ATCC VR-22) was obtained from the American Type Culture Collection (ATCC) and was adapted to Vero and H1299 cells. Virus stock was prepared as previously described (Liu et al., 2001). Titers of the virus stocks were determined by plaque assay on Vero or H1299 cells.

Measurement of cell proliferation and viability

Vero and H1299 cells were seeded in six-well plates at 10^5 cells per well. After 24 h of incubation, cells were mock-infected or infected with IBV at a multiplicity of infection (MOI) of 0.5 or 1 at 37 °C for 3 h. At various times post-infection, cells were harvested, resuspended in 2 ml of phosphate-buffered saline (PBS) and counted. The percentage of cell numbers at each time point was calculated by comparing with the mock-infected cells at 0 h post-infection.

MTT assay was carried out using the cell proliferation kit I (MTT) according to the manufacturer's recommended procedures (Roche Applied Science). Briefly, Vero and H1299 cells plated in 96-well plates at approximately 50% confluence were infected with IBV at an MOI of 1. At various times post-infection, 20 μl of MTT labeling reagent was added to each well and incubated at 37 °C for 4 h. After 150 μl of solubilization solution was added, the absorbance was measured at 550 nm in an enzyme-linked immunosorbent assay reader.

Cell cycle manipulation

Vero and H1299 cells were synchronized in the quiescent state by serum deprivation for 48 and 24 h, respectively. Approximately 3×10^5 cells were seeded into 6-mm dishes and maintained in medium without newborn calf serum for the indicated times. The synchronized cells were infected with IBV at an MOI of 1 as described above, and were analyzed by flow cytometry at indicated times post-infection.

For analysis of IBV replication in the S-phase, asynchronously growing H1299 cells in 48-well plates were treated with either DMSO or 20 μM methotrexate (Sigma-Aldrich) for 20 h, and incubated in fresh medium for 6 h afterwards. Cells were infected with IBV at an MOI of 1 and harvested at different times post-infection, followed by analysis of the cell cycle profiles, virus protein expression and viral titers. H1299 cells were synchronized at the G_1/S border using 20 μM of methotrexate.

Cell cycle analysis by flow cytometry

To determine cell cycle status, nuclear DNA content was measured by using propidium iodide staining and fluorescence-activated cell sorting (FACS) analysis. Briefly, cells were detached with trypsin and washed with PBS. The cell pellets were resuspended in 0.5 ml PBS containing 50 μg/ml propidium iodide and 100 μg/ml RNase, incubated at 4 °C for 30 min, and analyzed using a FACScan flow cytometer and ModFit LT Mac 3.0 software (BD Biosciences).

Western blot analysis

Polypeptides in cell lysates were separated by SDS–polyacrylamide gel electrophoresis, transferred to polyvinylidene difluoride membranes (Bio-Rad) by using a semi-dry transfer cell (Bio-Rad, Trans-blot SD), and blocked overnight at room temperature with 10% nonfat milk in PBS-T. The membrane was probed with primary antibodies followed by anti-mouse or anti-rabbit antibodies conjugated with horseradish peroxidase (Sigma). Membrane-bound antibodies were detected with either an enhanced chemiluminescence kit (Amersham) or a SuperSignal west pico chemiluminescence substrate kit (Pierce).

Antibodies against cyclin A (H-432), cyclin E (E-4), Cdk1 (17), Cdk2 (D-12), p21 (F-5), p27 (F-8), Ub (FL-76), fibrillarin (H-140) and β-tubulin (H-235) were purchased from Santa Cruz. Antibodies against cyclin B1 (V152) and cyclin D1 (DCS6) were obtained from Cell Signaling Technology. Antibody against RB (G3-245) was from BD Pharmingen and anti-p53 (Ab6) mouse monoclonal antibody was from Calbiochem. The polyclonal antibody against IBV N protein was generated in rabbit against the full-length N protein.

TUNEL assay

The terminal deoxynucleotidyltransferase-mediated dUTP-biotin nick end labeling (TUNEL) assay was performed with an *in situ* cell death detection kit, fluorescein, according to the protocol of the manufacturer (Roche). Briefly, cells were fixed with paraformaldehyde and permeabilized with Triton X-100 at room temperature. After equilibration, specimens were overlaid with 50 μl TUNEL reaction mixture and incubated in a humidified atmosphere for 60 min at 37 °C in the dark. Samples with the incorporated fluorescein were directly analyzed under a fluorescence microscope using an excitation wavelength of 488 nm.

Acknowledgments

This work was supported by the Agency for Science, Technology and Research, Singapore, and a grant from the Biomedical Research Council (BMRC 03/1/22/17/220), Agency for Science, Technology and Research, Singapore.

References

An, S., Chen, C.-J., Yu, X., Leibowitz, J.L., Markino, S., 1999. Induction of apoptosis in murine coronavirus-infected cultured cells and demonstration of E protein as an apoptosis inducer. J. Virol. 73, 7853–7859.

Barber, G.N., 2001. Host defense, viruses and apoptosis. Cell Death Differ. 8, 113–126.

Benedict, C.A., Norris, P.S., Ware, C.F., 2002. To kill or be killed: viral evasion of apoptosis. Nat. Immunol. 3, 1013–1018.

Chau, T.N., Lee, K.C., Yao, H., Tsang, T.Y., Chow, T.C., Yeung, Y.C., Choi, K.W., Tso, Y.K., Lau, T., Lai, S.T., Lai, C.L., 2004. SARS-associated viral hepatitis caused by a novel coronavirus: report of three cases. Hepatology 39, 302–310.

Chen, C.-J., Makino, S., 2004. Murine coronavirus replication induces cell cycle arrest in G_0/G_1 phase. J. Virol. 78, 5658–5669.

Chen, C.-J., Sugiyama, K., Kubo, H., Huang, H., Makino, S., 2004a. Murine coronavirus nonstructural protein p28 arrests cell cycle in G_0/G_1 phase. J. Virol. 78, 10410–10419.

Chen, W., Lee, J., Cho, S.Y., Fine, H.A., 2004b. Proteasome-mediated destruction of the cyclin A/cyclin-dependent kinase 2 complex suppresses tumor cell growth *in vitro* and *in vivo*. Cancer Res. 64, 3949–3957.

Chow, K.Y.C., Yeung, Y.S., Hon, C.C., Zeng, F., Law, K.M., Leung, F.C.C., 2005. Adenovirus-mediated expression of the C-terminal domain of SARS-CoV spike protein is sufficient to induce apoptosis in Vero E6 cells. FEBS Lett. 579, 6699–6704.

Cuconati, A., White, E., 2002. Viral homologs of BCL-2: role of apoptosis in the regulation of virus infection. Genes Dev. 16, 2465–2478.

DeCaprio, J.A., Ludlow, J.W., Lynch, D., Furukawa, Y., Griffin, J., Piwnica-Worms, H., Huang, C.M., Livingston, D.M., 1989. The product of the retinoblastoma susceptibility gene has properties of a cell cycle regulatory element. Cell 58, 1085–1095.

Desaintes, C., Goyat, S., Garbay, S., Yaniv, M., Thierry, F., 1999. Papillomavirus E_2 induces p53-independent apoptosis in HeLa cells. Oncogene 18, 4538–4545.

Dove, B., Brooks, G., Bicknell, K., Wurm, T., Hiscox, J.A., 2006. Cell cycle perturbations induced by infection with the coronavirus infectious bronchitis virus and their effect on viral replication. J. Virol. 80, 4147–4156.

Dyson, N., 1998. The regulation of E2F by pRB-family proteins. Genes Dev. 12, 2245–2262.

el-Deiry, W.S., Tokino, T., Velculescu, V.E., Levy, D.B., Parsons, R., Trent, J.M., Lin, D., Mercer, W.E., Kinzler, K.W., Vogelstein, B., 1993. WAF1, a potential mediator of p53 tumor suppression. Cell 75, 817–825.

Eleouet, J.F., Chilmonczyk, S., Besnardeau, L., Laude, H., 1998. Transmissible gastroenteritis coronavirus induces programmed cell death in infected cells through a caspase-dependent pathway. J. Virol. 72, 4918–4924.

Fan, X., Liu, Y., Chen, J.J., 2005. Down-regulation of p21 contributes to apoptosis induced by HPV E6 in human mammary epithelial cells. Apoptosis 10, 63–73.

Feuer, R., Mena, I., Pagarigan, R., Slifka, M.K., Whitton, J.L., 2002. Cell cycle status affects coxsackievirus replication, persistence, and reactivation in vitro. J. Virol. 76, 4430–4440.

Gil-Gomez, G., Berns, A., Brady, H.J., 1998. A link between cell cycle and cell death: Bax and Bcl-2 modulate Cdk2 activation during thymocyte apoptosis. EMBO J. 17, 7209–7218.

Gjoerup, O., Zaveri, D., Roberts, T.M., 2001. Induction of p53-independent apoptosis by simian virus 40 small antigen. J. Virol. 75, 9142–9155.

Goh, W.C., Rogel, M.E., Kinsey, C.M., Michael, S.F., Fultz, P.N., Nowak, M.A., Hahn, B.H., Emerman, M., 1998. HIV-1 Vpr increases viral expression by manipulation of the cell cycle: a mechanism for selection of Vpr in vivo. Nat. Med. 4, 65–71.

Groschel, B., Bushman, F., 2005. Cell cycle arrest in G_2/M promotes early steps of infection by human immunodeficiency virus. J. Virol. 79, 5695–5704.

Harbour, J.W., Dean, D.C., 2000. The Rb/E2F pathway: expanding roles and emerging paradigms. Genes Dev. 14, 2393–2409.

Harper, J.W., Adami, G.R., Wei, N., Keyomarsi, K., Elledge, S.J., 1993. The p21 Cdk-interacting protein Cip1 is a potent inhibitor of G1 cyclin-dependent kinases. Cell 75, 805–816.

Hay, S., Kannourakis, G., 2002. A time to kill: viral manipulation of the cell death program. J. Gen. Virol. 83, 1547–1564.

Helt, A.M., Harris, E., 2005. S-phase-dependent enhancement of dengue virus 2 replication in mosquito cells, but not in human cells. J. Virol. 79, 13218–13230.

Katz, R.A., Greger, J.G., Skalka, A.M., 2005. Effects of cell cycle status on early events in retroviral replication. J. Cell. Biochem. 94, 880–889.

King, K.L., Cidlowski, J.A., 1998. Cell cycle regulation and apoptosis. Annu. Rev. Physiol. 60, 601–617.

Kleinberger, T., 2000. Induction of apoptosis by adenovirus E4orf4 protein. Apoptosis 5, 211–215.

Ksiazek, T.G., Erdman, D., Goldsmith, C.S., Zaki, S.R., Peret, T., Emery, S., Tong, S., Urbani, C., Comer, J.A., Lim, W., Rollin, P.E., Dowell, S.F., Ling, A.E., Humphrey, C.D., Shieh, W.J., Guarner, J., Paddock, C.D., Rota, P., Fields, B., DeRisi, J., Yang, J.Y., Cox, N., Hughes, J.M., LeDuc, J.W., Bellini, W.J., Anderson, L.J., SARS Working Group, 2003. A novel coronavirus associated with severe acute respiratory syndrome. N. Engl. J. Med. 348, 1953–1966.

Kudoh, A., Daikoku, T., Sugaya, Y., Isomura, H., Fujita, M., Kiyono, T., Nishiyama, Y., Tsurumi, T., 2004. Inhibition of S-phase cyclin-dependent kinase activity blocks expression of Epstein–Barr virus immediate-early and early genes, preventing viral lytic replication. J. Virol. 78, 104–115.

Kudoh, A., Fujita, M., Zhang, L., Shirata, N., Daikoku, T., Sugaya, Y., Isomura, H., Nishiyama, Y., Tsurumi, T., 2005. Epstein–Barr virus lytic replication elicits ATM checkpoint signal transduction while providing an S-phase-like cellular environment. J. Biol. Chem. 280, 8156–8163.

Lai, M.M.C., Holmes, K.V., 2001. Coronaviridae: the viruses and their replication. In: Knipe, D.M., Howley, P.M. (Eds.), Fields Virology, vol. 1. 4th ed. Lippincott, Williams & Wilkins, Philadelphia, pp. 1163–1203.

Law, P.T.W., Wong, C.-H., Au, T.C.C., Chuck, C.P., Kong, S.K., Chan, P.K.S., To, K.-F., Lo, A.W.I., Chan, J.Y.W., Suen, Y.-K., Chan, H.Y.E., Fung, K.P., Waye, M.M.Y., Sung, J.J.Y., Lo, Y.M.D., Tsui, S.K.W., 2005. The 3a protein of severe acute respiratory syndrome-associated coronavirus induces apoptosis in Vero E6 cells. J. Gen. Virol. 86, 1921–1930.

Li, F.Q., Xiao, H., Tam, J.P., Liu, D.X., 2005. Sumoylation of the nucleocapsid protein of severe acute respiratory syndrome coronavirus. FEBS Lett. 579, 2387–2396.

Liu, C., Xu, H.Y., Liu, D.X., 2001. Induction of caspase-dependent apoptosis in cultured cells by the avian coronavirus infectious bronchitis virus. J. Virol. 75, 6402–6409.

Liu, Y., Cai, Y., Zhang, X., 2003. Induction of caspase-dependent apoptosis in cultured rRat oligodendrocytes by murine coronavirus is mediated during cell entry and does not require virus replication. J. Virol. 77, 11952–11963.

Luo, H., Zhang, J., Dastvan, F., Yanagawa, B., Reidy, M.A., Zhang, H.M., Yang, D., Wilson, J.E., McManus, B.M., 2003. Ubiquitin-dependent proteolysis of cyclin D1 is associated with coxsackievirus-induced cell growth arrest. J. Virol. 77, 1–9.

Macleod, K.F., Sherry, N., Hannon, G., Beach, D., Tokino, T., Kinzler, K., Vogelstein, B., Jacks, T., 1995. p53-dependent and independent expression of p21 during cell growth, differentiation, and DNA damage. Genes Dev. 9, 935–944.

Meikrantz, W., Gisselbrecht, S., Tam, S.W., Schlegel, R., 1994. Activation of cyclin A-dependent protein kinases during apoptosis. Proc. Natl. Acad. Sci. U.S.A. 91, 3754–3758.

Morgan, D.O., 1995. Principles of CDK regulation. Nature 374, 131–134.

Nurse, P., 2004. A long twentieth century of the cell cycle and beyond. Cell 100, 71–78.

Op De Beeck, A., Caillet-Fauquet, P., 1997. Viruses and the cell cycle. Prog. Cell Cycle Res. 3, 1–19.

Roulston, A., Marcellus, R.C., Branton, P.E., 1999. Viruses and apoptosis. Annu. Rev. Microbiol. 53, 577–628.

Santiago-Walker, A.E., Fikaris, A.J., Kao, G.D., Brown, E.J., Kazanietz, M.G., Meinkoth, J.L., 2005. Protein kinase C δ stimulates apoptosis by initiating G_1 phase cell cycle progression and S phase arrest. J. Biol. Chem. 280, 32107–32114.

Schang, L.M., 2003. The cell cycle, cyclin-dependent kinases, and viral infections: new horizons and unexpected connections. Prog. Cell Cycle Res. 5, 103–124.

Schmidt, M., Afione, S., Kotin, R.M., 2000. Adeno-associated virus type 2 Rep78 induces apoptosis through caspase activation independently of p53. J. Virol. 74, 9441–9450.

Scholle, F., Li, K., Bodola, F., Ikeda, M., Luxon, B.A., Lemon, S.M., 2004. Virus–host cell interactions during hepatitis C virus replication: impact of

polyprotein expression on the cellular transcriptome and cell cycle association with viral RNA synthesis. J. Virol. 75, 1513–1524.

Sherr, C.J., Roberts, J.M., 1999. CDK inhibitors: positive and negative regulators of G1-phase progression. Genes Dev. 13, 1501–1512.

Shivakumar, C.V., Brown, D.R., Deb, S., Deb, S.P., 1995. Wild-type human p53 transactivates the human proliferating cell nuclear antigen promoter. Mol. Cell. Biol. 15, 6785–6793.

Surjit, M., Liu, B., Jameel, S., Chow, V.-T.-K., Lal, S.K., 2004. The SARS coronavirus nucleocapsid protein induces actin reorganization and apoptosis in COS-1 cells in the absence of growth factors. Biochem. J. 383, 13–18.

Surjit, M., Liu, B., Chow, V.-T.-K., Lal, S.K., 2006. The nucleocapsid protein of severe acute respiratory syndrome-coronavirus inhibits the activity of cyclin–cyclin-dependent kinase complex and blocks S phase progression in mammalian cells. J. Biol. Chem. 281, 10669–10681.

Swanton, C., Jones, N., 2001. Strategies in subversion: deregulation of the mammalian cell cycle by viral gene products. Int. J. Exp. Pathol. 82, 3–13.

Tan, Y.-J., Fielding, B.C., Goh, P.-Y., Shen, S., Tan, T.H.P., Lim, S.G., Hong, W., 2004. Overexpression of 7a, a protein specifically encoded by the severe acute respiratory syndrome coronavirus, induces apoptosis via a caspase-dependent pathway. J. Virol. 78, 14043–14047.

Teodoro, J.G., Branton, P.E., 1997. Regulation of apoptosis by viral gene products. J. Virol. 71, 1739–1746.

Teodoro, J.G., Heilman, D.W., Parker, A.E., Green, M.R., 2004. The viral protein Apoptin associates with the anaphase-promoting complex to induce G_2/M arrest and apoptosis in the absence of p53. Genes Dev. 18, 1952–1957.

Vannucchi, S., Chiantore, M.V., Fiorucci, G., Percario, Z.A., Leone, S., Affabris, E., Romeo, G., 2005. TRAIL is a key target in S-phase slowing-dependent apoptosis induced by interferon-β in cervical carcinoma cells. Oncogene 24, 2536–2546.

Vogelstein, B., Lane, D., Levine, A.J., 2000. Surfing the p53 network. Nature 408, 307–310.

Weinberg, R.A., 1995. The retinoblastoma protein and cell cycle control. Cell 81, 323–330.

Yang, Y., Xiong, Z., Zhang, S., Yan, Y., Nguyen, J., Ng, B., Lu, H., Brendese, J., Yang, F., Wang, H., Yang, X.F., 2005. Bcl-xL inhibits T-cell apoptosis induced by expression of SARS coronavirus E protein in the absence of growth factors. Biochem. J. 392, 135–143.